Published in final edited form as:
Cancer Res. 2015 February 1; 75(3): 508–518. doi:10.1158/0008-5472.CAN-14-1215.

PD-1/SHP-2 inhibit Tc1/Th1 phenotypic responses and the activation of T cells in the tumor microenvironment

Jing Li[1], **Hyun-Bae Jie**[#2], **Yu Lei**[#2], **Neil Gildener-Leapman**[2], **Sumita Trivedi**[2], **Tony Green**[3], **Lawrence P. Kane**[4], and **Robert L. Ferris**[2,4,5]

[1]Department of Pharmacology and Pharmaceutical Sciences, School of Medicine, Tsinghua University, Beijing, China

[2]Department of Otolaryngology, University of Pittsburgh, Pittsburgh, PA, USA

[3]University of Pittsburgh Health Sciences

[4]Department of Immunology, University of Pittsburgh, Pittsburgh, PA, USA

[5]Cancer Immunology Program, University of Pittsburgh Cancer Institute, Pittsburgh, PA, USA

[#] These authors contributed equally to this work.

Abstract

Immune rejection of tumors is mediated by IFN-γ production and T cell cytolytic activity. These processes are impeded by PD-1, a co-inhibitory molecule expressed on T cells that is elevated in tumor-infiltrating lymphocytes (TIL). PD-1 elevation may reflect T cell exhaustion marked by decreased proliferation, production of type 1 cytokines and poor cytolytic activity. Although anti-PD-1 antibodies enhance IFN-γ secretion after stimulation of the T cell receptor (TCR), the mechanistic link between PD-1 and its effects on T cell help (Tc1/Th1 skewing) remains unclear. In prospectively collected cancer tissues, we found that TIL exhibited dampened Tc1/Th1 skewing and activation compared to peripheral blood lymphocytes (PBL). When PD-1 bound its ligand PD-L1 we observed a marked suppression of critical TCR target genes and Th1 cytokines. Conversely, PD-1 blockade reversed these suppressive effects of PD-1: PD-L1 ligation. We also found that the TCR regulated phosphatase SHP-2 was expressed higher in TIL than in PBL, tightly correlating with PD-1 expression and negative regulation of TCR target genes. Overall, these results defined a PD-1/SHP-2/STAT1/T-bet signaling axis mediating the suppressive effects of PD-1 on Th1 immunity at tumor sites. Our findings argue that PD-1 or SHP-2 blockade will be sufficient to restore robust Th1 immunity and T cell activation and thereby reverse immunosuppression in the tumor microenvironment.

Keywords

PD-1/SHP-2; T cell activation; anti-tumor immune response

To whom correspondence should be addressed: Robert L. Ferris, MD, PhD, Hillman Cancer Center Research Pavilion, 5117 Centre Avenue, Room 2.26b, Pittsburgh, PA USA 15213-1863, Phone: 412-623-0327, Fax: 412-623-4840, ferrisrl@upmc.edu.

There are no conflicts of interest.

Introduction

Although recent advances in surgery, chemotherapy and radiotherapy have been developed, the overall 5-year survival rate for head and neck squamous cell carcinoma (HNSCC) remains at about 50%. The tumor microenvironment in HNSCC patients is highly immunosuppressive, suggesting a potential to use immunotherapies to improve survival of HNSCC patients (1). One of the most important immune resistance mechanisms involves co-inhibitory pathways mediated by immune checkpoint receptors (ICRs), such as CTLA-4, PD-1, BTLA and LAG-3. These ICRs and their ligands are commonly overexpressed in the tumor microenvironment (2-6), suggesting a promising approach to activate anti-tumor immune response of T cells by blockade of ICRs (7). CTLA-4 antagonistic mAb (ipilimumab) has significant activity in patients with metastatic melanoma (8) and was approved by FDA in 2010 for melanoma. Anti-PD-1 mAbs have also demonstrated clinical efficacy in early-stage clinical trials for various tumor types and may provide durable anti-tumor responses (9). However, despite the clinical benefit of ICR antagonist antibodies, the mechanism of improved immune response is still poorly understood.

Optimal T cell-based anti-tumor immunity requires both Tc1-biased CD8+ T cells acting as cytolytic effector cells and CD4+ Th1 cells, to enhance the potency and duration of anti-tumor response. In response to IFN-γ and IL-12, STAT1 and STAT4 bind to the Tbx21 (encoding T-bet) enhancer and induce a T-bet dependent Tc1 response (including IFN-γ production and cytolytic development) in CD8+ T cells (10). Development of Th1 cells requires a multistep mechanism in which the transcription factors STAT1, T-bet and STAT4 are sequentially activated (11, 12). Sustained tumor regression that results from anti-tumor therapies such as cancer vaccines is dependent on a strong type 1 immune response. In contrast, CD4+ Th2 cells induce M2-biased tumor associated macrophages and suppress CD8+ anti-tumor response, driving a more tumor-permissive microenvironment (1). Therefore, skewing to a type 1-dominant tumor microenvironment is indispensable to enhance efficacy of anti-tumor immunotherapy.

Although blockade of the PD-1 pathway (PD-1/PD-L1) enhances production of IFN-γ (a hallmark Th1 cytokine) and cytolytic activity of tumor-infiltrating T cells in both tumor-bearing mice and cancer patients (13, 14), the link between PD-1 and type 1 immunity remains vague. After clustering with the T cell receptor for antigen (TCR) during inflammatory conditions, PD-1 can recruit the phosphatase SHP-2 (15, 16) and relieve SHP-2 from its auto-inhibited state (17). In contrast, blockade of PD-1 signaling inhibits phosphorylation of SHP-2 (18). We therefore hypothesized that PD-1 suppresses beneficial type 1-dominant immune responses in the tumor microenvironment through the PD-1/SHP-2/p-STAT1/T-bet axis. Stimulation of the T cell receptor (TCR) and CD28 would lead to activation of the PI3K/Akt/mTOR/p-S6 pathway, which is important for sustaining T cell survival and expansion (19). Thus, PD-1 might interfere with TCR/CD28 signaling to mediate the suppression of T cell survival and proliferation in cancer patients. In addition, PD-1 can turn off TCR/CD28 signals by inhibiting TCR-proximal kinases in T cells. In this study, we used unique, paired, freshly isolated tumor infiltrating lymphocytes (TIL) and peripheral blood lymphocytes (PBL) specimens to investigate the in vivo phenotypic and functional impact of PD-1 expression on TCR signaling and Th skewing directly in the

tumor microenvironment of cancer patients, since these TIL have appear to be more suppressed than in the peripheral circulation (2).

Materials and Methods

Patients and specimens

Peripheral blood samples and fresh tumor specimens were obtained from 41 patients with head and neck squamous cell carcinoma (HNSCC). All patients were seen in the Department of Otolaryngology at the University of Pittsburgh Medical Center, and all subjects signed an informed consent approved by the Institutional Review Board of the University of Pittsburgh (IRB# 99-06). The clinicopathological features of the HNSCC patients in this study are shown in Table 1. The patient cohort included 7 females and 34 males with a mean age of 58 years (range: 26~74 years).

Collection of peripheral blood mononuclear cells (PBMC) and tumor infiltrating lymphocytes (TIL)

Venous blood from HNSCC patients was drawn into heparinized tubes and centrifuged on Ficoll-Hypaque gradients (GE Healthcare Life Sciences, Piscataway, NJ). PBMC were recovered, washed in RPMI-1640 medium (Sigma, St. Louis, MO), and either used immediately for experiments or resuspended in freezing media containing 10% DMSO, transferred to Mr. Frosty containers (Thermo Scientific, Waltham, MA), and stored at −80°C until flow cytometry analysis. For TIL isolation, fresh tumors from HNSCC patients were minced into small pieces manually or using a gentleMACS Dissociator (Miltenyi Biotec, Auburn, CA), then transferred to 70 μm cell strainers (BD) and mechanically separated using the plunger of a 5-mL syringe. The cells passing through the cell strainer were collected and subjected to Ficoll-Hypaque gradient centrifugation. After centrifugation, mononuclear cells were recovered and stored at −80°C until flow cytometry analysis or immediately used for experiments.

Antibodies and flow cytometry

The following anti-human antibodies were used for staining: CD3-Alexa Fluor 700, FOXP3-PerCP/Cy5.5, phospho-STAT1 (pY701)-PE, phospho-STAT4 (pY693)-Alexa Fluor 488 and T-bet-BV711 purchased from BD Biosciences (San Jose, CA), CD3-PE-Cy7, PD-1-PerCP/Cy5.5, and CD25-PE-Cy7 purchased from Biolegend (San Diego, CA), CD8-PE-TR, CD4-PE-TR purchased from Life Technologies (Carlsbad, CA), PD-1-APC (Clone: MIH-4, eBioscience, San Diego, CA), phospho-S6 (Ser235/236)-Alexa Fluor 488 (Cell Signaling Technology, Danvers, MA), SH-PTP2 (C-18) (Santa Cruz Biotechnology, Dallas, TX) and APC-conjugated $F(ab')_2$ fragment goat anti-rabbit IgG (Jackson ImmunoResearch, West Grove, PA). Intracellular staining of FOXP3, SHP-2, p-STAT1, T-bet, p-STAT4 and p-S6 was performed as follows: PBMC or TIL were stained with surface marker antibodies, fixed with fixation/permeabilization buffer (eBioscience), washed, and stained for intracellular antigens in 1X permeabilization buffer. Cells were analyzed on an LSRFortessa (BD) or CyAn (Dako, Ft. Collins, CO) flow cytometer, and data analyzed using Flow Jo (Treestar, Ashland, OR) or Summit V4.3 software (Dako), respectively. The acquisition and analysis gates were restricted to the lymphocyte gate based on characteristic properties of the cells in

the forward and side scatter. Dead cells were excluded based on viability dye staining (Zombie Aqua Fixable Viability Dye, Biolegend).

Immunohistochemistry (IHC)

Formalin-fixed paraffin-embedded tissue sections were deparaffinized and dehydrated in xylene and graded ethanol solutions. Antigen retrieval was conducted in Tris-EDTA buffer. Immunoperoxidase stains were performed according to a standard protocol on the Ventana Benchmark Ultra platform. PD-L1 antibody was provided by Dr. Gordon Freeman at the Dana Farber Cancer Institute. PD-1 was stained using a mAb NAT105 at 1:500 titration. IFN-γ antibody was purchased from Abcam (Cambridge, MA) and incubated at 1:500 titration. Staining was interpreted by an oral and maxillofacial pathologist. Both the intensity and percentage of area of staining were evaluated. Representative pictures of matching areas were taken at 400×.

Re-stimulation of TIL using anti-CD3/-CD28/hIgG1 or anti-CD3/-CD28/PD-L1 beads

LEAF purified anti-human CD3 (clone UCHT1, Biolegend), LEAF purified anti-human CD28 (clone CD28.2, Biolegend) plus PD-L1-hIgG1 Fc fusion protein (R&D Systems, Minneapolis, MN) or control human IgG1 (Southern Biotech, Birmingham, AL) were covalently coupled to Dynabeads M-450 Epoxy beads according to the manufacturer's protocol (Life Technologies). We kept constant the total amount of protein at 5 μg per 10^7 beads as previously described (20). Generally, 10^7 beads were coated with 1 μg of anti-CD3 (20% of total protein), 1 μg of anti-CD28, and 60% of either PD-L1-hIGg1 Fc fusion protein or control human IgG1. Covalent coupling of the proteins to the beads was performed in 0.1 M sodium phosphate buffer for 24 h at room temperature with gentle tilting and rotation.

TIL were freshly isolated from tumor specimens and subjected to re-stimulation experiments. Total TIL were cultured with beads at a fixed cell: bead ratio of 1:10. Briefly, 0.5×10^6 TIL were plated in a 96-well U-bottom tissue culture plate with beads in 200 μL RPMI-1640 complete media in the presence of 100 μg/mL anti-PD-1 (BMS-936558) or hIgG4 isotype control provided by Bristol-Myers Squibb, or 50 μM fusaruside (6) as indicated. After 48 h incubation at 37°C with 5% CO_2, supernatants were collected and cells were stained and subjected to flow cytometry analysis.

Western Blot

Western blot was performed with phospho-SHP-2 (Tyr580) antibody (Cell Signaling Technology, Danvers, MA), SH-PTP2 Antibody (C-18) (Santa Cruz Biotechnology, Dallas, TX) and monoclonal anti-β-actin antibody (Sigma, St. Louis, MO).

Luminex assay

TIL culture supernatant levels of IFN-γ, TNF-α, IL-2, IL-4, IL-5 and IL-10 were tested using a human magnetic cytokine/chemokine panel 6-plex kit (Millipore, Billerica, MA) and analyzed by the UPCI Luminex Core Facility.

Statistical analysis

Averages were calculated as means. For non-parametric distribution of samples, P-values were calculated by Wilcoxon-Mann-Whitney tests using GraphPad Prism (GraphPad, La Jolla, CA). P-values < 0.05 were considered to be significant. *p<0.05, **p<0.01, ***p<0.001.

Results

TIL have dampened Tc1/Th1 phenotypic responses and activation status compared to PBL

To determine the status of Tc1/Th1 activation of T cells in the tumor microenvironment, we analyzed expression of p-STAT1, T-bet and p-STAT4 in T cells from paired peripheral blood lymphocytes (PBL) and tumor infiltrating lymphocytes (TIL) from head and neck squamous cell carcinoma (HNSCC) patients. Interestingly, $CD8^+$ TIL had significantly lower p-STAT1, T-bet and p-STAT4 expression at baseline (Figure 1A-B, p-STAT1: p=0.005; T-bet: p=0.0003 and p-STAT4: p=0.02), lower p-STAT1 and T-bet after TCR stimulation (Figure 1C-D, p-STAT1 and T-bet: p=0.03) compared to PBL, which also correlates with deficient expression of perforin in $CD8^+$ TIL (unpublished data). $CD4^+$ TIL possessed similar p-STAT1 and slightly higher T-bet but dramatically lower p-STAT4 at baseline (Figure 2A-B, T-bet: p=0.002 and p-STAT4: p=0.02), lower p-STAT1 and T-bet after TCR stimulation (Figure 2C-D, p-STAT1 and T-bet: p=0.03) compared to PBL. Foxp3- $CD4^+$ T cells also manifested a similar abortive Th1 differentiation program in TIL.

Next, we investigated the activation status of TIL marked by expression of phosphorylated ribosomal protein S6 (p-S6), a downstream target of the PI3K pathway (21). As expected, expression of p-S6 was significantly lower in $CD8^+$ and $CD4^+$ TIL than in PBL at baseline (Figure 1A-B and 2A-B, CD8: p=0.0001 and CD4: p=0.005) and post-stimulation (Figure 1C-D and Figure 2C-D, CD8, CD4: p=0.03), suggesting a dampened activation status of tumor infiltrating T cells, despite the presence of multiple tumor antigenic stimulus in the tumor microenvironment from which they were freshly isolated.

PD-1 suppresses TCR-stimulated upregulation of p-STAT1, T-bet and p-S6

Despite the fact that PD-L1, the major ligand for PD-1, is variably and heterogeneously expressed on HNSCC tumor cells (4 and Supplemental Figure 1), we observed co-localization of $PD\text{-}1^+$ TIL with $PD\text{-}L1^+$ tumor cells in vivo in the tumor microenvironment (Figure 3), indicating the PD-1 inhibitory signaling is relevant and functional in the tumor-infiltrating T cells. Having demonstrated impaired Tc1/Th1 responses and activation of TIL, we investigated whether PD-1 signaling could directly regulate p-STAT1 and T-bet, which are important regulators of the Th1 phenotype, in the tumor microenvironment. To explore this possibility, we generated anti-CD3/-CD28/PD-L1 or anti-CD3/-CD28/hIgG1 (control Ab) coated beads. Total TIL isolated from HNSCC patients were stimulated with these beads in the presence or absence of anti-PD-1 blockade (BMS-936558). Interestingly, TIL which highly expressed PD-1 showed lower p-STAT1 and T-bet, when stimulated with anti-CD3/-CD28/PD-L1 beads, than when stimulated with anti-CD3/-CD28/hIgG1 beads. This result indicates that PD-1 ligation with polyvalent PD-L1 suppresses upregulation of p-STAT1 and T-bet due to TCR stimulation. Additionally, anti-PD-1 blockade can restore p-

STAT1 and T-bet expression in TIL stimulated with anti-CD3/-CD28/PD-L1 beads (Figure 4A-C, p=0.02 and Supplemental Figure 2A-B), which suggests that inhibition of PD-1 signaling using a clinically effective blocking mAb could reverse the suppressive effects of PD-1 on Th1 phenotypic responses. However, anti-PD-1 blockade did not increase p-STAT1 or T-bet expression in TIL stimulated with anti-CD3/-CD28/hIgG1 (isotype control mAb) beads.

Next, we investigated whether PD-1 signaling interferes with signals downstream of TCR activation. Of interest, p-S6, which can be up-regulated by TCR signaling, was decreased by the ligation of PD-1 using PD-L1 coated beads. Consequently, blockade of PD-1 by anti-PD-1 Ab (BMS-936558) restored upregulation of p-S6 (Figure 4A and D, p=0.02 and Supplemental Figure 2C). These findings suggest that PD-1 signaling interferes with activation of downstream T cell activation molecules (such as p-S6) induced by TCR stimulation, promoting dysfunction of T cells in the tumor microenvironment.

PD-1 suppresses secretion of Th1 cytokines but not Th2 cytokines by TIL upon TCR stimulation

Since we observed that PD-1 could suppress p-STAT1 and T-bet, the transcription factors regulating production of Th1 cytokines by $CD8^+$ and $CD4^+$ T cells, we next investigated whether production of Th1 cytokines upon TCR stimulation is influenced by PD-1 ligation or anti-PD-1 blockade. Supernatants of TIL cultured with anti-CD3/-CD28/hIgG1 or anti-CD3/-CD28/PD-L1 beads for 48 hours, with or without anti-PD-1 blockade (BMS-936558), were analyzed by Luminex for Th1/Th2 cytokines secretion. As expected, secretion of the Th1 cytokines IFN-γ (p=0.008), TNF-α (data not shown) and IL-2 (p=0.02, p=0.04) was lower in TIL with anti-CD3/-CD28/PD-L1 stimulation, compared to those stimulated with anti-CD3/-CD28/hIgG1, while PD-1 blockade Ab could reverse the inhibitory effects of PD-1: PD-L1 ligation. Production of the Th2 cytokine IL-10 was not altered by PD-1 ligation or PD-1 blockade (Figure 4E). In order to validate our ex vivo findings in vivo, we conducted immunohistochemistry analysis of PD-1 and IFN-γ in serial sections of the original tumor tissues. When expression of PD-1 on TIL was high, the amount of IFN-γ in the tumor microenvironment was low (Tumor 1), and vice versa (Tumor 2, Figure 4F). Taken together, these findings suggest that PD-1 signaling negatively regulates Tc1/Th1 responses by suppressing activation of p-STAT1 and T-bet and secretion of Th1 cytokines.

SHP-2 is overexpressed in TIL, and strongly correlates with PD-1 expression

After ligand binding, PD-1 clusters with the TCR and can recruit SHP-2 to its immunoreceptor tyrosine-based switch motif (ITSM), where SHP-2 is phosphorylated (22). SHP-2 has been suggested to be a mediator of PD-1 inhibitory signals (23, 24). Since PD-1 is highly expressed in TIL (22, 24), we examined whether expression of SHP-2 itself correlates with PD-1 expression on TIL from HNSCC patients. Expression of SHP-2 was tested in paired PBL and TIL from HNSCC patients by flow cytometry. Although SHP-2 is ubiquitously expressed in T cells, the MFI of SHP-2 was significantly higher in TIL, compared with PBL (Figure 5A, CD8, CD4: p=0.002). In addition, the MFI of SHP-2 was even higher in $PD\text{-}1^+$ TIL than in $PD\text{-}1^-$ TIL (Figure 5B, CD8, CD4: p=0.002). We also observed that the levels of SHP-2 expression in tumor infiltrating T cells from HNSCC

patients positively correlated with PD-1 expression (Figure 5C, R^2=0.8643, p=0.02). Together, these observations strongly suggest that expression of SHP-2 correlates with PD-1 expression, particularly at the tumor sites.

SHP-2 activation by fusaruside suppresses p-STAT1/T-bet and production of Th1 cytokines

Because SHP-2 can function as a negative regulator of p-STAT1 in tumor cells (15) and lymphocytes (16), we next investigated whether activation of SHP-2 regulates the inhibitory effects of PD-1 signaling on p-STAT1 and T-bet. To investigate this possibility, we used fusaruside, a small-molecule compound that specifically induces phosphorylation of SHP-2 (16, 25) (Supplemental Figure 3), to activate SHP-2 directly in TIL, bypassing ligand engagement of PD-1. As shown in Figure 6A, upregulation of p-STAT1 and T-bet by TCR/CD28 stimulation was inhibited by fusaruside (50uM for 48hrs), even when the PD-1 signaling pathway was blocked (p=0.03). These results indicate that activation of SHP-2 suppresses p-STAT1 and T-bet in a fashion similar to PD-1 signaling. We also tested Th1/Th2 cytokines in the supernatants of TIL cultured in the presence or absence of fusaruside with TCR stimulation. Consistent with decreases in p-STAT1 and T-bet, activation of SHP-2 by fusaruside suppresses production of the Th1 cytokines IFN-γ (p=0.02, p=0.008), TNF-α (data not shown) and IL-2, but not the Th2 cytokine IL-10 (Figure 6B). Therefore, PD-1 appears to suppress Tc1/Th1 phenotypic responses that are controlled by p-STAT1/T-bet in the tumor microenvironment by recruiting and activating SHP-2 to skew away from a Th1-biased anti-tumor response.

Discussion

In this study, we provide a mechanistic explanation for how PD-1 suppresses type 1 immunity and T cell activation in the tumor microenvironment. First, we show that TIL which express significantly more PD-1 manifest dampened Tc1/Th1 phenotypic responses and activation status compared to T cells in PBL. Second, ligation of PD-1 to PD-L1 coated beads suppresses p-STAT1, T-bet, p-S6 and production of Th1 cytokines due to TCR stimulation, while an antagonist PD-1 mAb (BMS-936558) can reverse the negative effects of PD-1 signaling. Third, we demonstrate that SHP-2, the downstream mediator of PD-1, is increased in TIL and is tightly correlated with PD-1 expression. Furthermore, activation of SHP-2 by fusaruside can bypass PD-1 signaling to induce suppression of Tc1/Th1 phenotypic responses marked by expression of p-STAT1 and T-bet and secretion of Th1 cytokines. Taken together, our study describes a novel function for PD-1 in suppressing type 1 immunity, through inhibition of p-STAT1/T-bet, via SHP-2 activation, and in antagonizing TCR/CD28 signaling to decrease p-S6 expression.

Immune escape of tumors results from loss of tumor antigen expression (due to loss of expression of strong rejection antigens or loss of MHC class I molecules) (26, 27) and establishment of the immunosuppressive tumor microenvironment. Immunosuppression of effector T cells in the tumor microenvironment is mediated by increased expression of co-inhibitory receptors (such as PD-1 and CTLA-4) that inhibit activation of T cells, or by immunosuppressive cytokines (such as TGF-β and IL-10) derived from both tumor cells and

infiltrating Treg and MDSC (28-31). These inhibitory mechanisms are consistent with our observation of a dampened Th1/Tc1 phenotypic response in TIL (Figure 1 and 2).

In the ongoing clinical trials of anti-PD-1/PD-L1 therapies, there is discussion of whether clinical responses to PD-1/PD-L1 blockade correlate with PD-L1 expression on tumor cells or immune cells. Recently, a report on the clinical trial of anti-PD-1 mAb (BMS-936558) therapy in cancer patients showed that pre-treatment expression of PD-L1 on tumors was associated with enhanced clinical responses (9). In our re-stimulation system, anti-PD-1 blockade did not increase expression of p-STAT1 and T-bet or production of Th1 cytokines in TIL stimulated with anti-CD3/-CD28 alone. This might be because when we isolated TIL, PD-L1$^+$ tumor cells interacting with PD-1$^+$ TIL in the tumor microenvironment (Figure 3) were depleted, so that PD-1 ligands were much less abundant than in the tumor sites. Therefore, we might only observe beneficial effects of anti-PD-1 blockade on type 1 anti-tumor immunity when PD-L1 is re-introduced into the culture to mimic the real tumor microenvironment. Our findings also suggest an important role for PD-L1 expression on tumor cells in triggering PD-1 inhibitory signaling in the interacting T cells (Figure 4).

Type 1-biased innate effector cells (such as IL-12-producing DC and IFN-γ-producing NK/NKT cells) are crucial for inducing Th1 CD4$^+$ cells and Tc1 CD8$^+$ cells with optimal cytotoxicity and effector functions for tumor cell lysis. Adoptive transfer of Th1 cells (32) and antigen-specific Tc1 cells (33) elicits strong anti-tumor activity. In contrast, type-2 biased effector cells, which produce IL-4, IL-10 and TGF-β, negatively regulate type-1 anti-tumor immunity and make the tumor microenvironment more tumor-permissive. Thus, Th1/Tc1-biased anti-tumor immunity is highly desirable for rejection of tumors by the host immune system. Alteration of the Th1/Th2 balance should therefore be considered as a strategy for cancer immunotherapy, too.

PD-1 blockade has been shown to augment Th1 and Th17 responses (as evidenced by increased production of IFN-γ, IL-2, TNF-α, IL-6 and IL-17) and to suppress production of the Th2 cytokines IL-5 and IL-13 in reactivated T cells from peripheral blood of patients with prostate and advanced melanoma cancer (34). However, in our system, PD-1 signaling inhibits production of Th1 cytokines (IFN-γ, IL-2 and TNF-α) by TIL, without altering production of the Th2 cytokine IL-10 (Figure 4E). By contrast, IL-4 and IL-5, the other two Th2 cytokines, were below the limit of detection, indicating that they might not be actively produced by TIL even with TCR stimulation. We think the PD-1/SHP-2 signaling interferes with the Th1 skewing but not directly acts on Th2 differentiation. Fully differentiated Th2 phenotypes would not appear without some Th2-driving condition(s). Thus, PD-1 blockade appears to enhance Th1 responses but may not alter Th2 responses in the tumor microenvironment. In addition, in CT26 tumor-bearing mice, injection of anti-PD-L1 antibody induces higher levels of T-bet in CD8$^+$ TIL (35). What's more, phosphorylated SHP-2 can selectively sequester STAT1 from kinases that mediate phosphorylation and thus suppress the STAT1-dependent Th1 immune responses (16). Taken together, these findings suggest that Th1 immunity can be efficiently modulated by PD-1 or SHP-2.

In conclusion, anti-PD-1 blockade, which is being actively explored as an immunotherapy agent in clinical trials and has shown clinical efficacy in several solid tumors, can improve T

cell-based immunotherapy by restoring a robust type 1 anti-tumor immunity and enhancing T cell activation. Biomarkers of anti-PD-1 activity are needed to monitor the efficacy of this type of immunotherapy, which we suggest should include successful restoration of Th1 phenotypes. Additionally, SHP-2 inhibitory strategies might be a powerful tool for cancer immunotherapy. Thus, SHP-2 not only suppresses Tc1/Th1 skewing of tumor infiltrating T cells, but also inhibits pSTAT1-dependent expression of HLA/APM (elements of the antigen processing machinery), and secretion of T-cell attracting chemokines RANTES and IP10 (15) and the cytokine IL-12 (unpublished data) by head and neck cancer cells. Therefore, development of a specific SHP-2 inhibitor would be a promising strategy for cancer immunotherapy in the future.

Supplementary Material

Refer to Web version on PubMed Central for supplementary material.

Acknowledgements

PD-L1 Ab was a generous gift of Dr. Gordon Freeman, Dana-Farber Cancer Institute. We thank Dr. Renxiang Tan (Nanjing University, China) for generating and providing fusaruside (25) and also Dr. Yang Sun, Qiang Xu (Nanjing University, China) and Gang Liu (Tsinghua University, China) for generous assistance.

Supported by NIH grant R01 DE019727 and P50CA097190. This project used the UPCI Cancer Biomarkers Facility: Luminex Core Laboratory and Flow Cytometry Facility that are supported in part by award P30 CA047904. Jing Li is supported by the China Scholarship Council. Yu Lei is supported by T32 CA060397 (to R.L.F.) and NIH K99 DE024173.

References

1. Tong CC, Kao J, Sikora AG. Recognizing and reversing the immunosuppressive tumor microenvironment of head and neck cancer. Immunologic research. 2012; 54:266–74. [PubMed: 22454102]
2. Jie HB, Gildener-Leapman N, Li J, Srivastava RM, Gibson SP, Whiteside TL, et al. Intratumoral regulatory T cells upregulate immunosuppressive molecules in head and neck cancer patients. British journal of cancer. 2013; 109:2629–35. [PubMed: 24169351]
3. Salvi S, Fontana V, Boccardo S, Merlo DF, Margallo E, Laurent S, et al. Evaluation of CTLA-4 expression and relevance as a novel prognostic factor in patients with non-small cell lung cancer. Cancer Immunol Immun. 2012; 61:1463–72.
4. Lyford-Pike S, Peng S, Young GD, Taube JM, Westra WH, Akpeng B, et al. Evidence for a role of the PD-1:PD-L1 pathway in immune resistance of HPV-associated head and neck squamous cell carcinoma. Cancer research. 2013; 73:1733–41. [PubMed: 23288508]
5. Fourcade J, Sun Z, Pagliano O, Guillaume P, Luescher IF, Sander C, et al. CD8(+) T cells specific for tumor antigens can be rendered dysfunctional by the tumor microenvironment through upregulation of the inhibitory receptors BTLA and PD-1. Cancer research. 2012; 72:887–96. [PubMed: 22205715]
6. Woo SR, Turnis ME, Goldberg MV, Bankoti J, Selby M, Nirschl CJ, et al. Immune inhibitory molecules LAG-3 and PD-1 synergistically regulate T-cell function to promote tumoral immune escape. Cancer research. 2012; 72:917–27. [PubMed: 22186141]
7. Pardoll DM. The blockade of immune checkpoints in cancer immunotherapy. Nature reviews Cancer. 2012; 12:252–64.
8. Hodi FS, O'Day SJ, McDermott DF, Weber RW, Sosman JA, Haanen JB, et al. Improved survival with ipilimumab in patients with metastatic melanoma. The New England journal of medicine. 2010; 363:711–23. [PubMed: 20525992]

9. Topalian SL, Hodi FS, Brahmer JR, Gettinger SN, Smith DC, McDermott DF, et al. Safety, activity, and immune correlates of anti-PD-1 antibody in cancer. The New England journal of medicine. 2012; 366:2443–54. [PubMed: 22658127]
10. Yang Y, Ochando JC, Bromberg JS, Ding Y. Identification of a distant T-bet enhancer responsive to IL-12/Stat4 and IFNgamma/Stat1 signals. Blood. 2007; 110:2494–500. [PubMed: 17575072]
11. Thieu VT, Yu Q, Chang HC, Yeh N, Nguyen ET, Sehra S, et al. Signal transducer and activator of transcription 4 is required for the transcription factor T-bet to promote T helper 1 cell-fate determination. Immunity. 2008; 29:679–90. [PubMed: 18993086]
12. Wei L, Vahedi G, Sun HW, Watford WT, Takatori H, Ramos HL, et al. Discrete roles of STAT4 and STAT6 transcription factors in tuning epigenetic modifications and transcription during T helper cell differentiation. Immunity. 2010; 32:840–51. [PubMed: 20620946]
13. Nomi T, Sho M, Akahori T, Hamada K, Kubo A, Kanehiro H, et al. Clinical significance and therapeutic potential of the programmed death-1 ligand/programmed death-1 pathway in human pancreatic cancer. Clinical cancer research: an official journal of the American Association for Cancer Research. 2007; 13:2151–7. [PubMed: 17404099]
14. Badoual C, Hans S, Merillon N, Van Ryswick C, Ravel P, Benhamouda N, et al. PD-1-expressing tumor-infiltrating T cells are a favorable prognostic biomarker in HPV-associated head and neck cancer. Cancer research. 2013; 73:128–38. [PubMed: 23135914]
15. Leibowitz MS, Srivastava RM, Andrade Filho PA, Egloff AM, Wang L, Seethala RR, et al. SHP2 is overexpressed and inhibits pSTAT1-mediated APM component expression, T-cell attracting chemokine secretion, and CTL recognition in head and neck cancer cells. Clinical cancer research: an official journal of the American Association for Cancer Research. 2013; 19:798–808. [PubMed: 23363816]
16. Wu X, Guo W, Wu L, Gu Y, Gu L, Xu S, et al. Selective sequestration of STAT1 in the cytoplasm via phosphorylated SHP-2 ameliorates murine experimental colitis. Journal of immunology. 2012; 189:3497–507.
17. Hoff H, Brunner-Weinzierl MC. The tyrosine phosphatase SHP-2 regulates differentiation and apoptosis of individual primary T lymphocytes. European journal of immunology. 2007; 37:1072–86. [PubMed: 17330819]
18. Yamamoto R, Nishikori M, Kitawaki T, Sakai T, Hishizawa M, Tashima M, et al. PD-1-PD-1 ligand interaction contributes to immunosuppressive microenvironment of Hodgkin lymphoma. Blood. 2008; 111:3220–4. [PubMed: 18203952]
19. Sulic S, Panic L, Barkic M, Mercep M, Uzelac M, Volarevic S. Inactivation of S6 ribosomal protein gene in T lymphocytes activates a p53-dependent checkpoint response. Genes & development. 2005; 19:3070–82. [PubMed: 16357222]
20. Francisco LM, Salinas VH, Brown KE, Vanguri VK, Freeman GJ, Kuchroo VK, et al. PD-L1 regulates the development, maintenance, and function of induced regulatory T cells. The Journal of experimental medicine. 2009; 206:3015–29. [PubMed: 20008522]
21. Lee J, Su EW, Zhu C, Hainline S, Phuah J, Moroco JA, et al. Phosphotyrosine-dependent coupling of Tim-3 to T-cell receptor signaling pathways. Molecular and cellular biology. 2011; 31:3963–74. [PubMed: 21807895]
22. Chemnitz JM, Parry RV, Nichols KE, June CH, Riley JL. SHP-1 and SHP-2 associate with immunoreceptor tyrosine-based switch motif of programmed death 1 upon primary human T cell stimulation, but only receptor ligation prevents T cell activation. Journal of immunology. 2004; 173:945–54.
23. Wang SF, Fouquet S, Chapon M, Salmon H, Regnier F, Labroquere K, et al. Early T cell signalling is reversibly altered in PD-1+ T lymphocytes infiltrating human tumors. PloS one. 2011; 6:e17621. [PubMed: 21408177]
24. Yokosuka T, Takamatsu M, Kobayashi-Imanishi W, Hashimoto-Tane A, Azuma M, Saito T. Programmed cell death 1 forms negative costimulatory microclusters that directly inhibit T cell receptor signaling by recruiting phosphatase SHP2. The Journal of experimental medicine. 2012; 209:1201–17. [PubMed: 22641383]

25. Shu RG, Wang FW, Yang YM, Liu YX, Tan RX. Antibacterial and xanthine oxidase inhibitory cerebrosides from Fusarium sp. IFB-121, an endophytic fungus in Quercus variabilis. Lipids. 2004; 39:667–73. [PubMed: 15588024]
26. Ferris RL, Whiteside TL, Ferrone S. Immune escape associated with functional defects in antigen-processing machinery in head and neck cancer. Clinical cancer research: an official journal of the American Association for Cancer Research. 2006; 12:3890–5. [PubMed: 16818683]
27. Lopez-Albaitero A, Nayak JV, Ogino T, Machandia A, Gooding W, DeLeo AB, et al. Role of antigen-processing machinery in the in vitro resistance of squamous cell carcinoma of the head and neck cells to recognition by CTL. Journal of immunology. 2006; 176:3402–9.
28. Schreiber RD, Old LJ, Smyth MJ. Cancer immunoediting: integrating immunity's roles in cancer suppression and promotion. Science. 2011; 331:1565–70. [PubMed: 21436444]
29. Strauss L, Bergmann C, Gooding W, Johnson JT, Whiteside TL. The frequency and suppressor function of CD4+CD25highFoxp3+ T cells in the circulation of patients with squamous cell carcinoma of the head and neck. Clinical cancer research: an official journal of the American Association for Cancer Research. 2007; 13:6301–11. [PubMed: 17975141]
30. Jarnicki AG, Lysaght J, Todryk S, Mills KH. Suppression of antitumor immunity by IL-10 and TGF-beta-producing T cells infiltrating the growing tumor: influence of tumor environment on the induction of CD4+ and CD8+ regulatory T cells. Journal of immunology. 2006; 177:896–904.
31. Gabrilovich DI, Ostrand-Rosenberg S, Bronte V. Coordinated regulation of myeloid cells by tumours. Nat Rev Immunol. 2012; 12:253–68. [PubMed: 22437938]
32. Ikeda H, Chamoto K, Tsuji T, Suzuki Y, Wakita D, Takeshima T, et al. The critical role of type-1 innate and acquired immunity in tumor immunotherapy. Cancer science. 2004; 95:697–703. [PubMed: 15471553]
33. Dobrzanski MJ, Reome JB, Hylind JC, Rewers-Felkins KA. CD8-mediated type 1 antitumor responses selectively modulate endogenous differentiated and nondifferentiated T cell localization, activation, and function in progressive breast cancer. Journal of immunology. 2006; 177:8191–201.
34. Dulos J, Carven GJ, van Boxtel SJ, Evers S, Driessen-Engels LJ, Hobo W, et al. PD-1 blockade augments Th1 and Th17 and suppresses Th2 responses in peripheral blood from patients with prostate and advanced melanoma cancer. Journal of immunotherapy. 2012; 35:169–78. [PubMed: 22306905]
35. Duraiswamy J, Kaluza KM, Freeman GJ, Coukos G. Dual blockade of PD-1 and CTLA-4 combined with tumor vaccine effectively restores T-cell rejection function in tumors. Cancer research. 2013; 73:3591–603. [PubMed: 23633484]

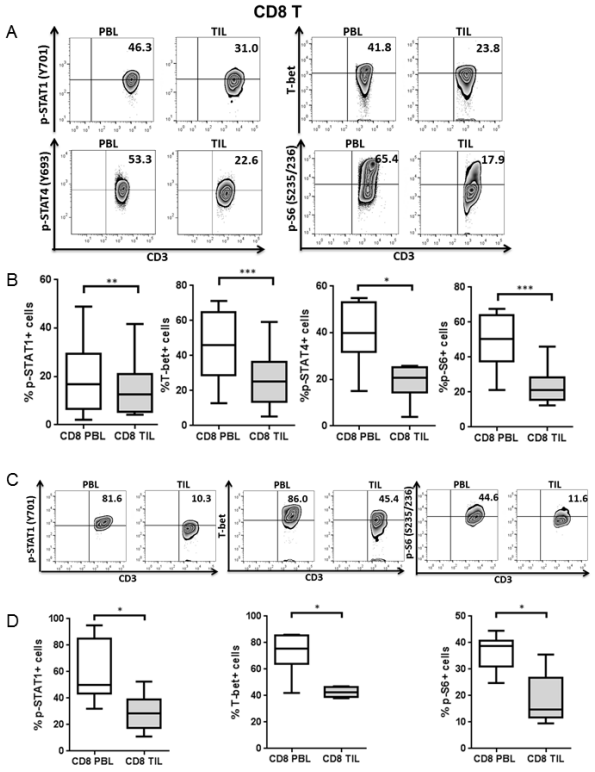

Figure 1. CD8$^+$ TIL have dampened Tc1 phenotypic responses and activation compared to PBL

p-STAT1, T-bet, p-STAT4 and p-S6 levels in CD8$^+$ PBL and TIL from HNSCC patients were analyzed by intracellular flow cytometry. Representative figures (A) and summary data (B) show percentage of p-STAT1 (Y701)+ (n=15), T-bet+ (n=16), p-STAT4 (Y693)+ (n=7) and p-S6 (S235/236)+ (n=13) cells in CD8$^+$ TIL compared with paired PBL at baseline. Total PBL and TIL were stimulated with anti-CD3/-CD28/hIgG1 beads (bead: cell= 10:1) for 48hrs and then p-STAT1, T-bet and p-S6 were tested by flow cytometry. Representative figures (C) and summary data (D) of percentage of p-STAT1 (Y701)+, T-bet+ and p-S6 (S235/236)+ (n=6) cells in CD8$^+$ TIL compared with paired PBL post-stimulation are shown. Statistical significance was determined by Wilcoxon (non-parametric paired) test. *p<0.05, **p<0.01, ***p<0.001.

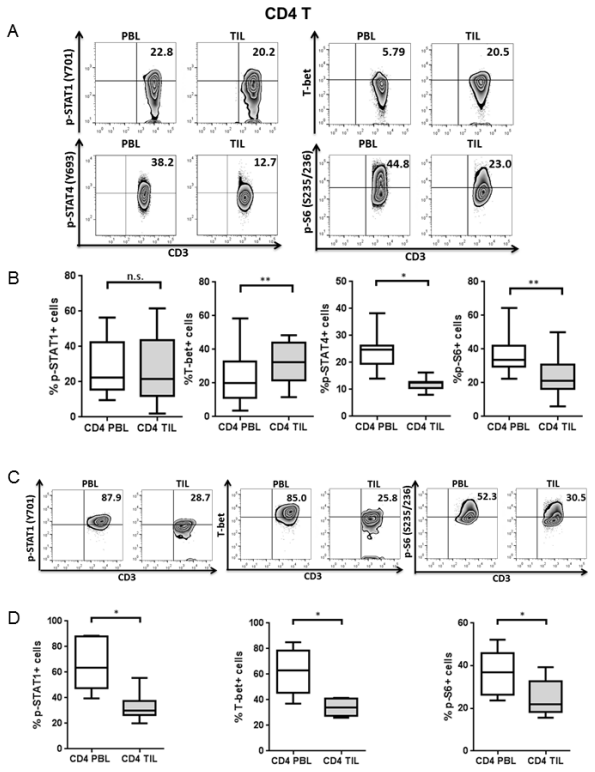

Figure 2. CD4$^+$ TIL show abortive Th1 differentiation and low activation compared with PBL

p-STAT1, T-bet, p-STAT4 and p-S6 levels in CD4$^+$ PBL and TIL from HNSCC patients were analyzed by intracellular flow cytometry. Representative figures (A) and summary data (B) show percentage of p-STAT1 (Y701)+ (n=15), T-bet+ (n=16), p-STAT4 (Y693)+ (n=7) and p-S6 (S235/236)+ (n=13) cells in CD4$^+$ TIL compared with paired PBL at baseline. Total PBL and TIL were stimulated with anti-CD3/-CD28/hIgG1 beads (bead: cell= 10:1) for 48hrs and then p-STAT1, T-bet and p-S6 were tested by flow cytometry. Representative figures (C) and summary data (D) of percentage of p-STAT1 (Y701)+, T-bet+ and p-S6 (S235/236)+ (n=6) cells in CD4$^+$ TIL compared with paired PBL post-stimulation are shown. Statistical significance was determined by Wilcoxon (non-parametric paired) test. *p<0.05, **p<0.01. p>0.05 was considered to be not significant (n.s.).

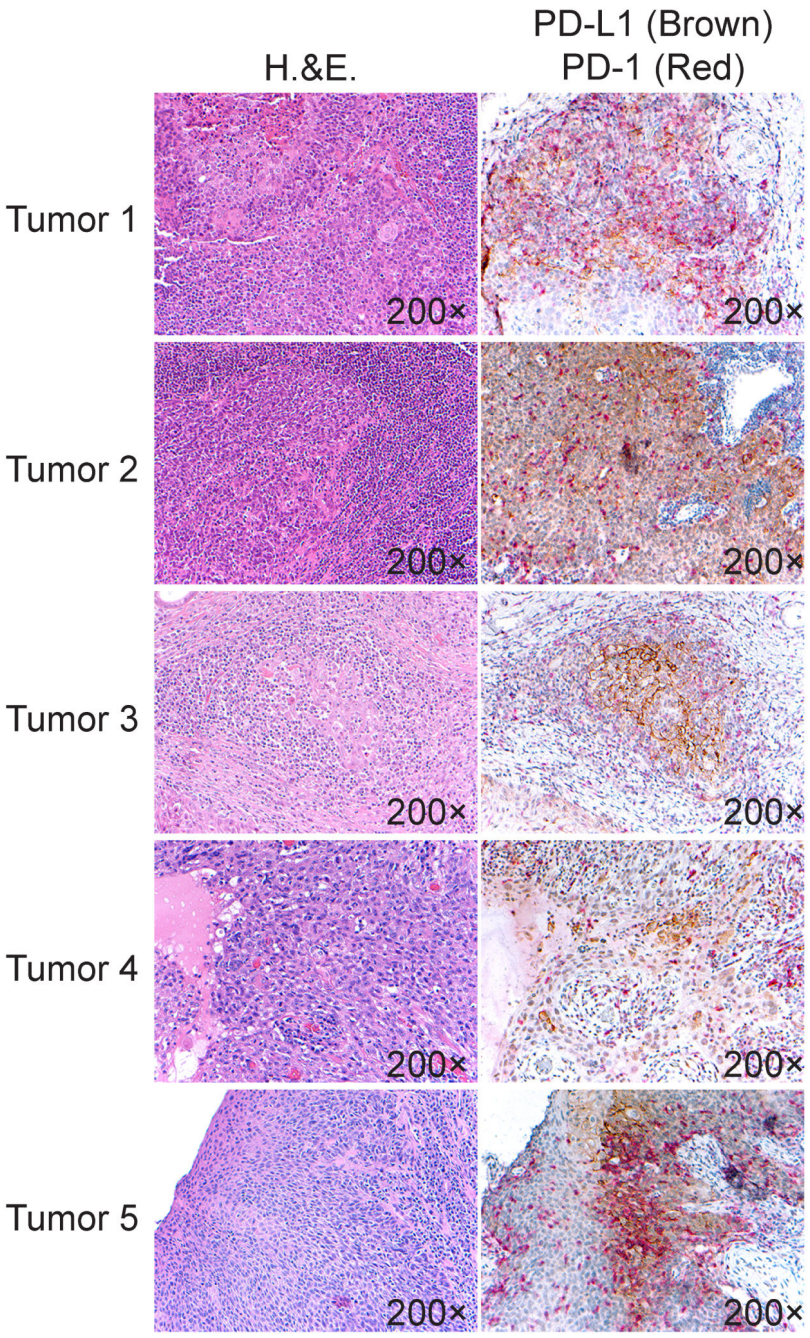

Figure 3. PD-1^{+} TIL co-localize with PD-L1^{+} HNSCC cells in the tumor microenvironment

H&E (left panels) and PD-1/PD-L1 double immunoperosidase staining (right panels) were performed, and representative matching areas in five (n=5) tumors are shown. PD-1-positive lymphocytes are labeled with a red chromogen, and PD-L1 positive HNSCC cells are labeled with a brown chromogen. Images were taken at 200×.

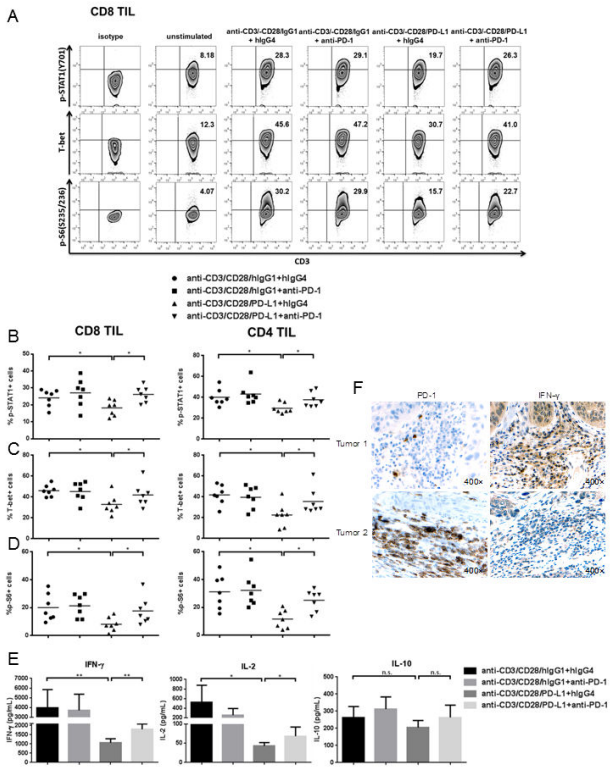

Figure 4. PD-1 ligation with bead-coated PD-L1 suppresses p-STAT1, T-bet, p-S6 and production of Th1 cytokines upon TCR stimulation, while anti-PD-1 blockade could reverse the suppressive effects of PD-1

Total TIL were stimulated with anti-CD3/-CD28/hIgG1 or anti-CD3/-CD28/PD-L1 coated beads (bead: cell=10:1) for 48h in the presence of 100ug/mL hIgG4 or anti-PD-1 (BMS-936558), then p-STAT1, T-bet and p-S6 were analyzed by flow cytometry. Supernatants from each condition were collected and stored at −80°C. Th1 (IFN-γ and IL-2) and Th2 (IL-10) cytokines in the supernatants were determined by Luminex. A) Representative data showing p-STAT1 (Y701), T-bet and p-S6 (S235/236) levels in $CD8^+$ TIL under the described conditions. Summary data of frequency of p-STAT1 (Y701)+ (B), T-bet+ (C) and p-S6 (S235/236)+ (D) in $CD8^+$ and $CD4^+$ TIL with indicated conditions is shown (n=7). E) Summary data of amount of IFN-γ, IL-2 and IL-10 in the supernatants of TIL cultured under indicated conditions is shown. The graphs present the mean ± SEM from 8 HNSCC patients. F) Immunohistochemistry analysis of PD-1 and IFN-γ in serial sections of representative HNSCC tumors. Statistical significance was determined by Wilcoxon (non-parametric paired) test. *$p<0.05$, **$p<0.01$. $p>0.05$ was considered to be not significant (n.s.).

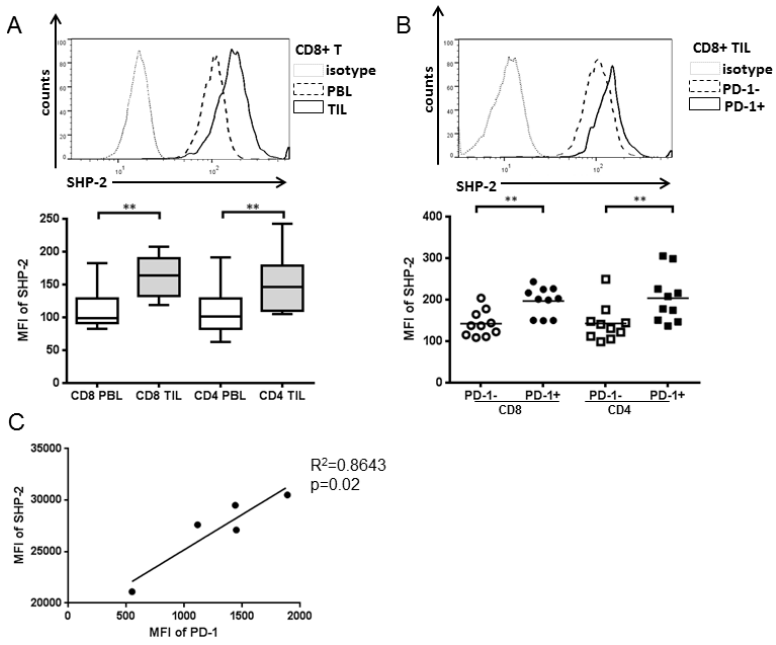

Figure 5. SHP-2 is overexpressed in TIL and correlates with PD-1$^+$ expression

Expression level of SHP-2 in TIL and paired PBL from HNSCC patients (n=10) was assessed by flow cytometry. A) Representative figure (upper panel) and summary data (lower panel) showing MFI of SHP-2 in CD8$^+$ and CD4$^+$ TIL compared with PBL. B) Representative figure (upper panel) and summary data (lower panel) showing MFI of SHP-2 in PD-1$^-$ and PD-1$^+$ CD8$^+$ and CD4$^+$ TIL. Statistical significance was determined by Wilcoxon (non-parametric paired) test. **p<0.01. C) Expression levels of PD-1 and SHP-2 (shown by MFI) in tumor infiltrating T cells from 5 HNSCC patients.

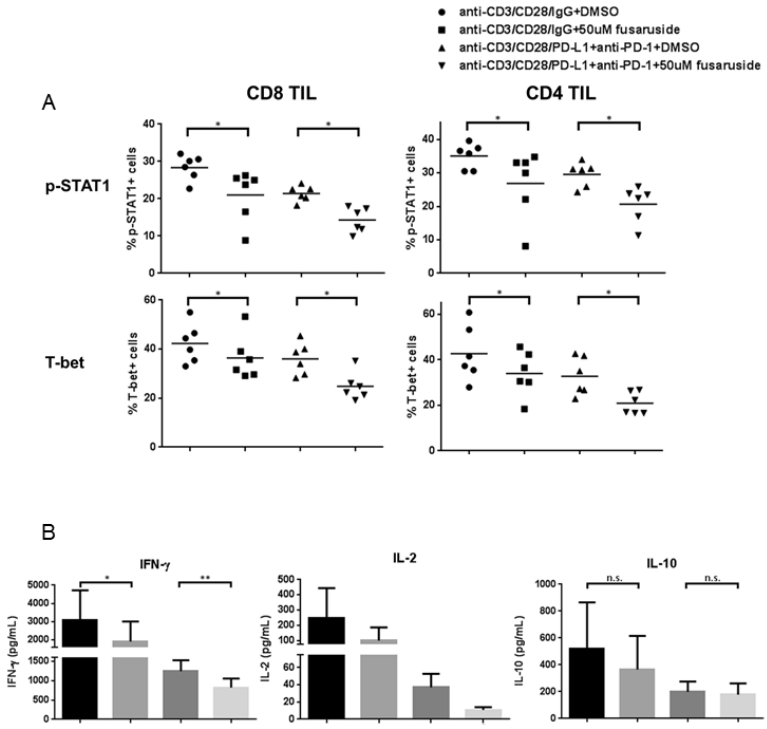

Figure 6. SHP-2 activation by fusaruside suppresses p-STAT1/T-bet and production of Th1 cytokines upon TCR stimulation

Total TIL were stimulated with anti-CD3/-CD28/hIgG1 beads (bead: cell=10:1) or anti-CD3/-CD28/PD-L1 beads plus 100ug/mL anti-PD-1 blockade (BMS-936558) for 48h in the presence of 50uM fusaruside or DMSO. Then p-STAT1 and T-bet were analyzed by flow cytometry. Supernatants were collected and stored at −80°C. Th1 (IFN-γ and IL-2) and Th2 (IL-10) cytokines in the supernatants were determined by Luminex. A) Summary data of frequency of p-STAT1+ and T-bet+ cells in $CD8^+$ and $CD4^+$ TIL at different conditions is shown (n=6). B) Summary data of amount of IFN-γ (n=8), IL-2 (n=4) and IL-10 (n=8) in the supernatants of TIL cultured under indicated conditions. The graphs present the mean ± SEM from different HNSCC patients. Statistical significance was determined by Wilcoxon (non-parametric paired) test. *$p<0.05$, **$p<0.01$. $p>0.05$ was considered to be not significant (n.s.).

Table 1

Clinicopathological features of the patients with head and neck cancer in this study

Patient	Gender	Age	Tumor site	T-Stage, Path	N-stage, Path	M-stage, Path
1	Female	62	OC	T4A	N0	MX
2	Male	71	L	T4A	N0	MX
3	Male	54	OC	T2	N0	MX
4	Female	68	OC	T1	N0	MX
5	Male	72	OC	T4A	N0	MX
6	Male	50	L	T4A	N2C	MX
7	Male	57	OC	T4A	N3	M0
8	Male	63	OC	T2	N0	M0
9	Male	61	L	T3	N0	MX
10	Male	59	OP	T2	N2B	MX
11	Female	53	L	T3	N2B	MX
12	Female	69	OC	T4	N2C	MX
13	Male	58	OC	T4A	N2B	MX
14	Male	54	OC	T2	N2C	MX
15	Male	49	L	T4A	N2B	MX
16	Male	68	OP	T4A	N1	MX
17	Male	52	L	T4A	N1	MX
18	Male	26	OC	T2	N2B	MX
19	Male	63	OC	T2	N0	M0
20	Female	56	L	TX	N0	MX
21	Male	54	OC	T4A	N2C	MX
22	Male	68	OC	T4A	N0	MX
23	Male	59	L	T3	N0	M0
24	Male	52	OC	T4A	N0	MX
25	Male	58	OP	TX	NX	MX
26	Male	49	L	T3	N0	MX
27	Female	69	OP	TX	N1B	MX
28	Male	74	OP	T1	N2B	MX
29	Male	69	OC	T4A	N1	MX
30	Male	64	OP	T1	N0	MX
31	Male	46	OP	T2	N2B	MX
32	Male	54	OP	T2	N2A	MX
33	Male	47	L	T2	N2A	MX
34	Male	56	OC	T3	N0	M0
35	Male	60	OC	T2	N0	M0
36	Male	61	OC	N/A	N/A	N/A

Patient	Gender	Age	Tumor site	T-Stage, Path	N-stage, Path	M-stage, Path
37	Male	44	OP	T1	N2B	M0
38	Female	72	OC	T4A	N0	MX
39	Male	71	OC	T4A	N1	MX
40	Male	51	OP	N/A	N/A	N/A
41	Male	42	n/a	N/A	N/A	N/A

Abbreviation: OC, oral cavity; OP, oropharynx; L, larynx